Published in final edited form as:
Exp Neurol. 2009 March ; 216(1): 207–218. doi:10.1016/j.expneurol.2008.11.019.

Neuritic Dystrophy and Neuronopathy in Akita (*Ins2*^{Akita}) Diabetic Mouse Sympathetic Ganglia

Robert E. Schmidt, **Karen G. Green**, **Lisa L. Snipes**, and **Dongyan Feng**
Division of Neuropathology, Department of Pathology and Immunology, Washington University School of Medicine, Saint Louis, Missouri, USA, 63110

Abstract

Diabetic autonomic neuropathy is a debilitating, poorly studied complication of diabetes. Our previous studies of non-obese diabetic (NOD) and related mouse models identified rapidly developing, dramatic pathology in prevertebral sympathetic ganglia; however, once diabetic, the mice did not survive for extended periods needed to examine the ability of therapeutic agents to correct established neuropathy. In the current manuscript we show that the Akita (*Ins2*^{Akita}) mouse is a robust model of diabetic sympathetic autonomic neuropathy with unambiguous, spontaneous, rapidly-developing neuropathology which corresponds closely to the characteristic pathology of other rodent models and man. Akita mice diabetic for 2, 4 or 8 months of diabetes progressively developed markedly swollen axons and dendrites ("neuritic dystrophy") in the prevertebral superior mesenteric (SMG) and celiac ganglia (CG). Comparable changes failed to develop in the superior cervical ganglia (SCG) of the Akita mouse or in any ganglia of non-diabetic mice. Morphometric studies demonstrate an overall increase in presynaptic axon terminal cross sectional area, including those without any ultrastructural features of dystrophy. Neurons in Akita mouse prevertebral sympathetic ganglia show an unusual perikaryal alteration characterized by the accumulation of membranous aggregates and minute mitochondria and loss of rough endoplasmic reticulum. These changes result in the loss of a third of neurons in the CG over the course of 8 months of diabetes. The extended survival of diabetic mice and robust pathologic findings provide a clinically relevant paradigm that will facilitate the analysis of novel therapeutic agents on the reversal of autonomic neuropathy.

Keywords

diabetes; Akita mouse; neuritic dystrophy; neuronopathy; degeneration; sympathetic ganglia

INTRODUCTION

Autonomic neuropathy is an increasingly recognized problem in human diabetes which may result in a variety of complaints involving cardiovascular, genitourinary, sudomotor and alimentary symptoms (Rundles, 1945) or result in subclinical disease. Studies of prevertebral sympathetic ganglia in autopsied diabetic human subjects demonstrate neuroaxonal dystrophy

Please address correspondence to: Robert E. Schmidt, MD, PhD, Department of Pathology and Immunology (Box 8118), Washington University School of Medicine, 660 South Euclid Avenue, Saint Louis, MO 63110, (314) 362-7429 FAX: (314) 362-4096, Email: E-mail: reschmidt@wustl.edu.

(NAD) (Duchen et al., 1980; Schmidt et al., 1993), an axonopathy represented by marked enlargement of distal axons containing a distinctive admixture of cytoskeletal, autophagic, vesicular and membranous elements. Immunohistochemical studies are consistent with the origin of NAD from other sympathetic neurons (Schmidt, 2002), possibly as the result of intraganglionic sprouting. These axonopathic changes are accompanied by a mild, poorly characterized decrease in neuronal density (Schmidt et al., 1993). Nerve terminal damage is likely to dis- or misconnect ganglionic neurons and, particularly for prevertebral ganglia serving the viscera, contribute to the loss of integrated reflexes. Rat models of diabetic sympathetic autonomic neuropathy show correspondence with human pathology, developing dystrophic axons in prevertebral ganglia (Schmidt, 2002) in the absence of significant neuronal loss (Schmidt, 2001). The fidelity of animal models to the neuropathology of aged and diabetic humans suggests that similar pathogenetic mechanisms may be involved with a comparable response to experimental therapeutic approaches.

Previously we have shown that non-obese diabetic (NOD) mice or streptozotocin-treated NOD/severe combined immune deficient (STZ-Rx NOD/SCID) mice develop dramatic axonal as well as dendritic pathology (thus designated “neuritic dystrophy”) within a few weeks of onset of diabetes (Schmidt et al., 2003). Our recent studies with these models (Schmidt et al., in press) have shown that there is a continuum of ultrastructural changes in identified presynaptic axon terminals in diabetic mouse sympathetic ganglia which begin with early alterations in synaptic vesicle content and morphology and culminate in the development of anastomosing tubulovesicular membranous aggregates in swollen preterminal axons and formation of multivesicular autophagic bodies. Using STZ-treated NOD/SCID mice, we were able to show that erythropoietin and carbamylated erythropoietin prevented the development of experimental diabetic autonomic neuropathy (Schmidt et al., 2008). Unfortunately, NOD and STZ-treated NOD/SCID mice, once diabetic, do not survive for extended periods needed to determine the ability of therapeutic agents to correct established neuropathy, clinically a more relevant paradigm than prevention of the neuropathy. We have previously shown that STZ-treatment of B6D2F1, C57BL6, DBA/2J and BL6/NCR strains of mice resulted in neuritic dystrophy identical in ultrastructural appearance and anatomic distribution to that in NOD or STZ-Rx NOD/SCID mice (Schmidt et al., 2003). However, the pace of development of neuritic dystrophy in these strains is significantly slower and the ultimate severity of neuritic dystrophy limited in comparison to NOD and STZ-Rx NOD/SCID mice (e.g., 5 months of STZ-induced diabetes in C57BL6 mice produced 7-fold fewer dystrophic neurites than NOD mice diabetic for 5 weeks).

In search of a better mouse model we examined the Akita (*Ins2*^{Akita}) mouse in which a spontaneous dominant mutation in the insulin 2 gene on a C57BL6 mouse background results in replacement of cysteine with tyrosine at position 96. This substitution disrupts a disulfide bridge required for proper insulin folding, resulting in initiation of the unfolded protein response and pancreatic β-cell apoptosis in the absence of obesity, insulitis or insulin resistance (Yoshioka et al., 1997; Mathews et al., 2002; Ron, 2002; Izumi et al., 2003). Heterozygous Akita mice become reproducibly and severely hyperglycemic and hypoinsulinemic at 3–4 weeks of age but remain fertile and viable in the absence of exogenous insulin treatment. The diabetic phenotype is more severe and progressive in the Akita male than in the female. Akita mice are relatively hardy and maintain marked hyperglycemia comparable in severity to that of NOD and STZ-Rx NOD/SCID mice for durations up to 8 months, far longer than 5–8 weeks of severe hyperglycemia which can be maintained in NOD and NOD/SCID models in which animals become debilitated and fragile. Recent studies of chronically diabetic Akita mice have shown diabetic complications including gait disturbance and sensory neuropathy as well as progressive retinopathy (Choeiri et al., 2005; Barber et al., 2005). In anticipation of initiating studies of novel therapeutic agents, in this manuscript we have characterized the neuropathology of sympathetic autonomic ganglia in Akita diabetic and age-matched controls

diabetic for 2–8 months. We demonstrate that male Akita-diabetic mice show marked neuritic dystrophy in prevertebral sympathetic ganglia identical in appearance and anatomic distribution to that which develops in other mouse models. The frequency of neuritic dystrophy is substantial in Akita mice after only 2 months of diabetes and is progressive over the next 6 months. In addition, neurons in Akita mouse prevertebral sympathetic ganglia show an unusual perikaryal alteration characterized by the accumulation of membranous aggregates and minute mitochondria and loss of rough endoplasmic reticulum culminating in neuronal degeneration.

MATERIALS AND METHODS

Animals

The C57BL/6J-Ins2Akita animals used in the currently reported studies were obtained from the Jackson Laboratory. All animals were housed and cared for in accordance with the guidelines of the Washington University Committee for the Humane Care of Laboratory Animals and with National Institutes of Health guidelines on laboratory animal welfare. All mice were allowed standard rat chow and water ad libitum and maintained on a 12/12 hour light/dark cycle.

Tissue Preparation

Animals were anesthetized with ketamine/xylazine and perfused with 25 ml of heparinized saline followed by 25 ml of modified Karnovsky's fixative containing 3% glutaraldehyde and 1% paraformaldehyde in sodium cacodylate buffer pH 7.4. Fixation was continued overnight at 4°C in the same fixative and the following day the superior mesenteric (SMG), celiac (CG) and superior cervical (SCG) ganglia were dissected, cleaned of extraneous tissue and rinsed in sodium cacodylate buffer. Tissue was postfixed in phosphate cacodylate-buffered 21% OsO_4 for 1 hour, dehydrated in graded ethanols with a final dehydration in propylene oxide and embedded in EMbed-812 (Electron Microscopy Sciences, Hatfield, PA). One micron thick plastic sections were examined by light microscopy after staining with toluidine blue. Ultrathin sections (90 nanometers thick) of individual ganglia were cut onto formvar coated slot grids, which permits visualization of entire ganglionic cross sections. Sections were post stained with uranyl acetate and Venable's lead citrate and viewed with a JEOL model 1200EX electron microscope (JEOL, Tokyo, Japan). Digital images were acquired using the AMT Advantage HR (Advanced Microscopy Techniques, Danvers, MA).

Morphometric Studies

Determination of the Cross Sectional Area of Presynaptic Axon Terminals— Sections of entire SMG, CG or SCG were examined by an observer blinded to the identity of individual animals. Ganglia were systematically scanned at 20,000× magnification beginning at one tissue margin scanning vertical columns, from left to right until the entire ganglionic cross section had been examined. We identified individual synaptic active zones (defined by the presence of pre- and postsynaptic densities with immediately adjacent collections of synaptic vesicles) as synapses irrespective of the size or the nature of subcellular organelles composing their associated presynaptic axon terminal, reasoning that identifying active zones, which did not differ in size in ganglia of diabetic and age-matched control mice, would not significantly bias the analysis by over representing large presynaptic nerve terminals. Images of the entire axonal terminal associated with individual active zones were captured at 40,000× magnification irrespective of their contents, i.e., including both dystrophic and normal subcellular elements. The cross sectional area of presynaptic axonal terminals was determined using imageJ software and expressed as microns^2. Approximately 40–50 synapses were captured from each ganglionic cross section.

Quantitation of Dystrophic Neurites—Dystrophic elements are typically intimately related to neuronal perikarya and, therefore, we routinely express their frequency as the ratio of numbers of lesions to numbers of nucleated neuronal cell bodies. This method, used in our previous studies (Schmidt et al., 2003; Schmidt et al., 2008), substantively reduced the variance in assessments of intraganglionic lesion frequency. In addition, its simplicity permits the quantitative ultrastructural examination of relatively large numbers of ganglia and identification of robust changes. In the presence of neuron loss this method may overestimate the frequency of neuritic dystrophy, although loss of principal sympathetic neurons, thought to be the source of intraganglionic dystrophic neurites, may conversely result in parallel changes in dystrophic neurites and neuron number and an unchanged ratio. In our current animal studies an entire cross section of the SMG, CG or SCG was scanned at 20,000× magnification and the number of dystrophic neurites and synapses was determined by an investigator blinded to the identity of individual animals. Dystrophic neurites consist of swollen axons, synapses, dendritic spines or dendrites containing a variety of organelles including: 1) axonal tubulovesicular aggregates; 2) pallid ribosome poor cytoplasm in dendrites; 3) axons with admixed normal and degenerating subcellular organelles and multivesicular bodies; 4) axonal neurofilaments; and, 5) nearly pure aggregates of minute dendritic mitochondria. The number of nucleated neurons (range: 50–100 neurons examined in each ganglionic cross section) was determined simultaneously. The frequency of ganglionic neuritic dystrophy was expressed as the ratio of number of dystrophic neurites to the number of nucleated neurons in the same cross section.

Determination of Numbers of Pale Neuronal Cell Bodies—Numbers of cell bodies with pale cytoplasm (as shown in the Results section, Figs 1E–G) were determined in blinded fashion by light microscopy using 1000X oil immersion and expressed as the number of pale neurons as a percentage of the total number of nucleated cell bodies for each mouse.

CG Neuronal Counts—Male Akita mice diabetic for 8 months and age-matched C57BL/6J controls were killed by decapitation after ketamine/xylazine anesthesia. The CG were dissected and stored at −80°C. Ganglia were subsequently thawed and fixed overnight in 4% paraformaldehyde, processed through graded alcohols and embedded in paraffin. Sections were taken sequentially at 5 micron thickness to include the entire ganglion. Paraffin sections were stained with hematoxylin and eosin. Neuronal counts were made using the method described by Silos-Santiago et al. (2005) from every 3rd section. The numbers of neurons were determined by counting only cells with an obvious nucleus containing one or more nucleoli using a 60X objective on a Olympus BX51 photomicroscope. In order to correct for split nuclei, approximately 4–6 fields containing approximately 100 nucleolated neurons total were collected randomly from each diabetic and control ganglion using an Olympus DP70 digital camera and the same area from the consecutive section were photographed. The number of nuclei with nucleoli appearing on two successive sections were counted. We found that the number of nucleolated nuclei which appeared in both fields was 7.2% ± 0.8 (controls) and 7.4% ± 1.1 (Akita). Therefore, the final number of CG neurons was estimated by multiplying the raw data by the correction factor, 0.96 which was the same in controls and Akita mice.

Statistical Analysis

Statistical analysis was performed using a two tailed T-test.

RESULTS

Metabolic Parameters

Akita mice were received at 6–8 weeks of age and initial blood glucose values were determined showing all animals were diabetic at that point (blood glucose values >300 mg/dl). Diabetic

animals and age-matched C57BL6 control mice were killed at 2, 4, and 8 months of diabetes. Body weights of diabetics were significantly less than controls at 4 and 8 months and blood glucose values were significantly increased (Table 1).

Neuropathology of Sympathetic Ganglia

Light Microscopic Examination—Examination of 1 micron thick plastic sections of SMG and CG of 2, 4 and 8 month diabetic Akita and age-matched C57BL6 controls showed large and small principal sympathetic neurons surrounded by neuropil composed of an admixture of axons, dendrites and mast cells (Fig 1). Neurons of control ganglia had prominent nuclei, nucleoli and Nissl substance which extended more or less uniformly from the nucleus to the plasmalemma (Fig 1A).

Prevertebral ganglia from Akita mice showed pathologic changes in animals diabetic from 2 to 8 months. Scattered swollen neurites, represented by collections of glassy or granular cytoplasm (arrow, Fig 1B), were typically located immediately adjacent to neuronal cell bodies, often within their satellite cell sheaths, which resulted in displacement and distortion of perikaryal contours of targeted neurons. Similar dystrophic swellings were not observed by light microscopic examination in SMG or CG of non-diabetic control mice.

Examination of neuronal perikarya of Akita mice showed a continuum of degenerative changes. Patchy loss of Nissl substance (arrow, Fig 1C) commonly involved areas immediately adjacent to the plasmalemmal membrane or were more perinuclear and central (arrows, Fig 1D), or, in some cases, involved the entire perikaryon (arrow, Fig 1E). Later changes in neurons involved the accumulation of densely stained cytoplasmic bodies (arrow, Fig 1F) or, very rarely, frankly degenerating cell bodies (arrow, Fig 1G). Quantitation of pale neurons showed they represented 5–7% of total numbers of neurons at 4 months of diabetes and were also present, although at significantly decreased frequency, at 2 and 8 months of diabetes (Table 2). Thus, although cumulative neuronal loss may worsen with duration of diabetes, the progression of the process may not be uniform or may involve subpopulations of neurons dropping out between 4 and 8 months of diabetes. Morphometric analysis of 4 month diabetic SMG revealed a significant increase in the cross sectional area of principal sympathetic neurons (Controls: 354 ± 4 microns^2, n=46 + 10 neurons measured from each of 3 mice; Akita: 400 + 8 microns^2, n=57 ± 14 neurons measured from each of 5 mice, $p<0.003$). Pale neurons were never observed by light microscopic examination of non-diabetic age-matched controls.

In order to determine the fate of pathologically altered neurons we determined the number of neurons in the CG of Akita mice diabetic for 8 months and age-matched controls. Akita mice showed the loss of 33% of neurons from the CG over this period of time (Controls: 3238 ± 92 neurons, n=6 mice; Akita: 2116 ± 88 neurons, n=5 mice, $p\leq0.0001$).

In Chinese hamsters, NOD mice, STZ- and genetically-diabetic rats and man there is a dramatic, as yet unexplained, difference in the frequency of neuritic dystrophy between heavily involved prevertebral SMG and CG and the SCG, the largest of the paravertebral chain ganglia, which are minimally involved. Light microscopic examination of one micron plastic sections of Akita and control SCG similarly failed to show pale neurons or dystrophic swellings (data not shown).

Ultrastructural Examination

Ultrastructural examination of neuronal perikarya confirmed and extended light microscopic findings. The distribution of rough endoplasmic reticulum in control SMG and CG neurons was uniform (Fig 2A,B), with the exception of scattered patches of Golgi complex, and extended from the nucleus to the plasmalemma. The nuclear contours and nucleoplasm of

control neurons was also uniform with one or several nucleoli and relatively little heterochromatin. Akita mice diabetic from 2–8 months showed pale unstructured patches of perikaryal subplasmalemmal cytoplasm (arrow, Figs 2C,D) in which organelles, particularly rough endoplasmic reticulum, were lacking but appeared otherwise unremarkable. A pale neuron (arrow, Figs 2E,F) shows general loss of rough endoplasmic reticulum and the presence of smaller mitochondria than an adjacent normal appearing neuronal perikaryon (arrowheads, Figs 2E,F).

Many pale neurons contained additional pathologic findings (Fig 3) compared to adjacent neurons (Fig 3A). Prominent were whorled collections of membranes (arrow, Figs 3B,C), large numbers of smaller mitochondria than those in adjacent non-involved perikarya (arrows, Fig 3B) and numerous tubulovesicular elements (arrows, Fig 3D) which may represent residual endoplasmic reticulum largely devoid of ribosomes. In addition there are irregularities in nuclear contours, granular nucleoplasm and increased heterochromatin (Fig 3A,E). Similar changes can be seen extending into the proximal neurites of pale neurons (arrow, Fig 3E). Finally, neurons may be completely replaced by accumulated membranous whorls, degenerating mitochondria and autophagosomes (Fig 3F).

Ultrastructural examination also demonstrated numerous swollen dystrophic elements in the SMG and CG of Akita mice diabetic for 2, 4 and 8 months (Fig 4) which were rare in non-diabetic age-matched controls. Dystrophic neurites were typically completely enclosed within the cytoplasm of Schwann or satellite cells (arrow, Fig 4A) and frequently separated from adjacent perikarya by interposed satellite cell processes. As in our previously published mouse studies (Schmidt et al., 2003) dystrophic neurites exhibited a variety of ultrastructural patterns based on differences in their content of subcellular organelles. A striking pattern (arrow, Fig 4B), which involved 18–20% of all dystrophic elements in 4 month diabetic SMG and CG, consisted of neurites, mostly axons, containing normal and degenerating organelles, an appearance dominated by the accumulation of autophagosomes (Fig 4B) as well as admixtures of organelles and a disoriented microtubular cytoskeleton (Figs 4C,D). The most typical dystrophic appearance (43–45% of the total number of dystrophic neurites) consisted of collections of large numbers of mitochondria which were tightly aggregated without a significant amount of intervening cytoplasm (arrows, Fig 4E). The majority of mitochondria filled neurites involved dendrites, as identified by synapses ending upon them, the presence of ribosomes or lipopigment. Numerous dystrophic swellings (33–36%) contained large numbers of coarse to delicate tubulovesicular elements, some with clefts. Occasional neurites (1–2% of the total), typically axons, contained aggregates of neurofilaments. Collections of swollen lucent neurites (arrowhead, Fig 4E) containing pale cytoplasm and small mitochondria (Fig 4F) likely represent the terminal portions of projections from pale neuronal perikarya, although we have not confirmed continuity ultrastructurally.

The rare examples of dystrophic neurites in SMG and CG of control mice were identical in appearance to diabetics, including forms containing tubulovesicles, autophagosomes and mitochondria. Dystrophic neurites were extraordinarily rare in the SCG of 4 month diabetic Akita.

Quantitative analysis of the Frequency of Neuritic Dystrophy—Since dystrophic neurites were present in both diabetic and, although quite rarely, in control mice, we thought it necessary to apply an ultrastructural quantitative method to accurately compare them and to determine if the frequency of dystrophy was progressive with duration of diabetes. The numbers of dystrophic neurites were counted as described in the Materials and Methods section and expressed as a ratio (numbers of dystrophic elements/numbers of nucleated neurons). This analysis established that dystrophic neurites were markedly increased in the diabetic Akita mice at each duration of diabetes compared with age-matched controls (Table 3). Both 4 month

diabetic SMG and CG showed comparable numbers of dystrophic neurites (Table 3): however, neuritic dystrophy was several orders of magnitude less frequent in the SCG (Table 3). Although the numbers of dystrophic neurites is increased in 8 month diabetic Akita mice compared to 4 month diabetics, the loss of neuronal cell bodies may have artificially enhanced the frequency of dystrophy expressed as a ratio of dystrophic neurites to neuronal number.

Quantitative Analysis of Cross Sectional Area of Presynaptic Axon Terminals— Our recent studies (Schmidt et al., in press) of NOD, STZ-Rx NOD/SCID and STZ-Rx C57BL6 mice show increased cross sectional area of synapses in comparison to age-matched non-diabetic controls. Although presynaptic axon terminals (arrows, Fig 5A) vary in size in normal mice, Akita mouse synapses frequently were comparatively large and engorged with synaptic vesicles (Fig 5B). We measured the cross sectional area of all presynaptic terminal axons forming synapses (defined as collections of synaptic vesicles at an active zone with pre and post-synaptic densities) encountered in the CG cross section of animals diabetic for 4 and 8 months of diabetes and age-matched controls (Table 4). We found a 48–55% increase in axonal terminal cross sectional area in Akita mice CG compared to age-matched controls. Size-frequency histograms (Fig 4) show a general shift from a predominance of small axon terminals in non-diabetic control CG to larger forms in CG of Akita mice diabetic for 8 months. This pattern is seen in both SMG and CG of Akita mice. The presynaptic axon termini in the paravertebral SCG of Akita diabetic mice showed a 27% decrease or no change in 4 and 8 month diabetic mice, respectively (Table 4).

DISCUSSION

Comparison of Mouse Models of Diabetic Sympathetic Autonomic Neuropathy

We have examined the development of sympathetic autonomic neuropathy in several different mouse models. Although the NOD mouse rapidly develops dramatic neuropathology within 3–5 weeks of onset of diabetes, NOD mice develop diabetes spontaneously over a time course which may range from 12–30 weeks of age; therefore, NOD mice with the same duration of diabetes may actually represent animals which differ significantly in age. Unfortunately, the necessity of using the NOD background inbred strain complicates the practical application of the NOD model to the wealth of available mice with transgenic or spontaneous mutations and knockouts of selected genes which have been generated on a variety of other genetic backgrounds. The ability to synchronize the development of diabetes by STZ-treatment of NOD/SCID mice, which fail to spontaneously develop islet inflammation and destruction as the result of defects in B and T cells, represents a significant advantage over the NOD model. However, neither diabetic NOD or STZ-Rx NOD/SCID mice survive for more than 5–6 weeks after the onset of diabetes making it difficult to test novel therapeutic agents after the development of diabetic autonomic neuropathy, a reversal paradigm most comparable to anticipated use in clinical diabetes. The necessity of breeding NOD/SCID strain mice with the variety of animals with selected spontaneous or genetically engineered mice in order to induce diabetic autonomic neuropathy diminishes their utility. Additionally, the increase in the baseline frequency of neuritic dystrophy in non-diabetic NOD/SCID sibs suggests that these control animals may not be entirely normal. Recent work (Chaparro et al., 2006) shows untreated NOD/SCID mice (i.e., the “controls” for STZ-treated NOD/SCID mouse experiments) have normal to low blood glucose levels and higher circulating insulin levels when compared with other inbred strains of mice. Surprisingly, NOD/SCID mice have defects in glucose homeostasis, insulin response and proteosome-dependent ubiquitination mediated protein degradation, the latter possibly resulting in the accumulation of debris in neuritic processes. Various strains of mice (B6D2F1, C57BL6, DBA/2J and BL6/NCR) made diabetic with STZ, a paradigm which might be used to induce diabetes in mice with spontaneous or induced gene defects, typically develop less severe hyperglycemia and fewer (but

ultrastructurally identical) dystrophic neurites over a much longer time course (4–5 months compared to 3–5 weeks) compared to NOD and STZ-Rx NOD/SCID mice. The db/db mouse is an exception, failing to develop neuritic dystrophy in the presence of hyperglycemia, a result thought to reflect increased levels of IGF-I and insulin operating as neurotrophic substances (Schmidt et al., 2003).

The Akita mouse model offers significant advantages over these previously examined mouse models. Akita mice develop neuritic dystrophy comparable ultrastructurally and in anatomic distribution to these previously characterized in other mouse models (Schmidt et al., 2003). Male Akita mice reproducibly develop severe diabetes between the third and fourth week of life. The severity and time course of neuropathology in the Akita mouse resembles the fast pace of dramatic neuritic dystrophy in NOD and STZ-Rx NOD/SCID mice compared to the slower development in STZ-induced diabetic strains of mice. In contrast, Akita mice are capable of long survival (more than 8 months in our animal facility) once they become severely diabetic which will permit the analysis of the effect of novel therapeutic agents used on established neuritic dystrophy, i.e., in a more clinically relevant reversibility paradigm. The explanation for the differences in the survival of Akita mice in comparison to NOD and STZ-induced NOD/SCID mouse models is unknown. Additionally, the non-diabetic C57BL6/J parent strain of Akita mice exhibits very little baseline neuritic dystrophy, differing importantly from the variable, frequently high background levels in some strains (e.g., non-diabetic NOD/SCID mice).

Neuronopathy—Akita mice show clear evidence of a continuum of neuronal cell body pathology beginning as patchy loss of rough endoplasmic reticulum, through the accumulation of distinctive membranous aggregates and culminating in neuronal degeneration. This pattern of neuron loss is not apoptotic with its characteristic nuclear fragmentation, has only a few features of autophagy based degeneration and is reminiscent of guanethidine-induced sympathetic degeneration in neonatal rats (Schmidt et al., 1990). Although degenerating sympathetic neurons are not as prominent in other diabetic mouse models as in Akita mice, we have encountered individual neurons containing similar membranous aggregates as well as rare (<1%) pale neurons in STZ-induced diabetic C57BL6 mice (unpublished data). Perikaryal structural changes are striking in the SMG and CG of the Akita mouse and result in the loss of approximately a third of CG neuron loss over 8 months.

Additionally, there is both peripheral and central loss of rough endoplasmic reticulum, i.e., peripheral or central chromatolysis, respectively, although there is only modest swelling of the cell body or peripheral displacement of the nucleus, changes which typically accompany classic central chromatolysis. It remains possible, but as yet unproven, that the dystrophic structural changes in the distal axons and dendrites in the Akita mouse SMG and CG (and their absence in the SCG) reflect dysfunctional early alterations in the cell bodies of SMG and CG neurons, possibly resulting in defects in maintaining axonal transport and synaptic structure. The lack of membrane bound ribosomes in dendritic processes is particularly poised to contribute to the loss of plasticity in dendrites and dendritic spines.

The significance of changes in the number and size of mitochondria in the neuronal cell body and dendrites is unknown; however, recent studies have identified a significant role for a dynamic network of mitochondrial fission and fusion in the determination of mitochondrial number, size and function which may contribute to a variety of neurodegenerative processes (Baloh, 2008; Chan, 2006; Frank, 2006). It is possible that the accumulation of small mitochondria in perikaryal and dendritic sites reflects foci of increased energy demand since mitochondria are known to fuse and divide (Karbowski and Youle, 2003) at sites of energy demand in response to ATP/ADP gradients. Large aggregates of axonal mitochondria have also been identified in DRG of diabetic rats in vivo and in DRG cultured in high glucose media,

a result proposed to result from the upregulation of the fission-related protein Drp1 (Leinninger et al., 2006). Expression of neuropathy-associated forms of the fusion inducing protein MFN2 in cultured DRG neurons induced defects in axonal transport of mitochondria resulting in abnormal clustering of small fragmented mitochondria in both neuronal cell bodies and proximal axons (Baloh et al., 2007; Baloh, 2008).

Morphologic changes in the sympathetic neuronal cell bodies have been inconspicuous in our human and experimental rat models. Early studies of sympathetic ganglia in diabetic patients reported enlargement of neurons including giant or vacuolated forms (Hopfner et al., 1971; Appenzeller and Richardson, 1966; Budzilovich, 1970; Kott et al., 1974), although some apparent perikaryal enlargement may have been complicated by the presence of granular dystrophic terminals (Schmidt, 1996) previously interpreted as part of the neuronal perikaryon. Our early human studies demonstrated a small (~14%) decrease in neuronal density (Schmidt et al., 1993) in the prevertebral sympathetic ganglia of diabetic patients. However, it is difficult to reproducibly sample such large human plexiform ganglia with indistinct borders and, as a result, non-biased counting methods have not been used in analysis of human diabetic sympathetic ganglia. Thus, the true incidence or degree of neuron loss in human sympathetic ganglia is not established. Although chronic STZ-diabetic rat prevertebral and paravertebral sympathetic ganglia subjected to non-biased counting methods fail to show neuron loss (Schmidt, 2001), the neuronopathy found in Akita mice is not a typical finding in STZ-induced diabetic rat sympathetic ganglia. Similarly, loss of 10–20% of DRG neurons in diabetic mice is in contrast to neuronal preservation in STZ-diabetic rat DRG (Zochodne et al., 2008).

Dendritic Elements: Although our early human studies failed to identify dendritic swellings in diabetic human subjects, it is likely that only the most proximal dendritic swellings would have been identified with silver histochemical stains and even MAP-2 immunostaining (Schmidt et al., 1993; Schmidt et al., 1997). We have not identified dystrophic swellings in mouse, rat, Chinese hamster and humans originating from the juxtaneuronal axon or dendrites. Afferents to sympathetic ganglia primarily form synapses on dendritic spines and dendrites compared to cell bodies (Forehand, 1985) and changes in dendritic size or structure may substantially influence neuronal function since the extent of the dendritic arbor permits the integration of many weak inputs from diffuse sources (Parkman et al., 1994). It is known that the size of the dendritic arbor plays an important role in determining the number of axonal terminals forming synapses on a principal sympathetic neuron (Purves and Lichtman, 1985). Involvement of both axonal terminals and terminal dendrites in diabetic sympathetic ganglia could reasonably be expected to significantly impair organized neuronal responses.

SCG vs. SMG and CG—The distribution of neuritic dystrophy, increased synaptic cross sectional area and neuronopathy in the Akita mouse selectively involves prevertebral sympathetic ganglia, i.e., SMG and CG, with nearly complete sparing of the SCG, the largest and most rostral member of the paravertebral sympathetic chain ganglia. This pattern of involvement is shared with diabetes in rat, Chinese hamster and man as well as NOD mice. A variety of studies have also shown differences between prevertebral and paravertebral ganglia in electrophysiology, morphology, immunohistochemistry, sensitivity to NGF deprivation and response to guanethidine sympathectomy (Hill, 1985; Hill et al., 1985; Schmidt et al., 1988; Jobling and Gibbins, 1999). Our recent studies of mutant mice lacking the calcium independent phospholipase A2β (*iPLA2β*) gene also show marked neuroaxonal dystrophy in sympathetic ganglia (Malik et al., 2008), which is similarly confined to the SMG and CG, sparing the SCG. In that study we proposed that altered membrane composition, reflecting changes in classes of lipid molecules, could result in membrane instability and interference with membrane recycling ultimately resulting in dystrophic changes. Gene microarray studies (Carroll et al., 2004) have also demonstrated marked differences in SCG and SMG-CG in rats diabetic for 2–6 weeks (prior to the development of structural dystrophy in rats). Prevertebral SMG/CG showed

substantial diabetes-induced differences in comparison with the SCG in the same animals, particularly involving structural and functional synaptic constituents and encoding proteins related to oxidative stress, paralleling the eventual distribution of structural dystrophic changes in the ganglia and their distal projections.

The marked heterogeneity in the response of different sympathetic ganglia to a variety of clinical and experimental insults remains unexplained. There are differences in the response of sympathetic ganglia of diabetic rats to treatment with the antioxidant α-lipoic acid which corrects the diabetes-induced decrease of cardiac norepinephrine (derived from the paravertebral SCG and stellate chain ganglia) but not that in the ileum which is chiefly prevertebral in origin (Shotton et al., 2003). Recent work by Lincoln and colleagues using established sympathetic neuron cultures, has shown that exposure to high levels of glucose decreased the frequency of neurite-bearing CG/SMG neurons but did not affect SCG neurons (Semra et al., 2004). CG/SMG neurons showed a decrease in anti-oxidant defense enzyme activity with lesser total superoxide dismutase and glutathione peroxidase activity (Semra et al., 2004), a result which may explain the greater effect of the oxidant stressor menadione on CG/SMG than SCG neurons (Semra et al., 2006).

Summary

Our results establish the Akita mouse as a robust model of diabetic autonomic neuropathy. The Akita mouse develops sympathetic autonomic neuropathy with unambiguous, spontaneous, rapidly-developing neuropathology which corresponds closely to the characteristic pathology of other rodent models and man. The distinctive neuronopathy may provide additional insights into the pathogenesis of neuritic changes in distal dendrites and axon terminals. Spontaneously diabetic Akita mice quickly develop severe sympathetic ganglionic neuropathology which is progressive over the 8 month time course we have examined. These characteristics may permit the rapid determination of the effect of therapeutic agents given in both preventative and interventional paradigms as well as testing a variety of proposed pathogenetic mechanisms.

Acknowledgements

NIH awards R37 DK19645 and AG10299; Juvenile Diabetes Research Foundation Grants 1-2005-1085 and 1-2008-193

References

Appenzeller O, Richardson EP Jr. The sympathetic chain in patients with diabetic and alcoholic polyneuropathy. Neurology 1966;16:1205–1209. [PubMed: 4162684]

Baloh RH. Mitochondrial dynamics and peripheral neuropathy. Neuroscientist 2008;14:12–18. [PubMed: 17911220]

Baloh RH, Schmidt RE, Pestronk A, Milbrandt J. Altered axonal mitochondrial transport in the pathogenesis of Charcot-Marie-Tooth disease from mitofusin 2 mutations. J Neurosci 2007;27:422–430. [PubMed: 17215403]

Barber AJ, Antonetti DA, Kern TS, Reiter CE, Soans RS, Krady JK, Levison SW, Gardner TW, Bronson SK. The Ins2Akita mouse as a model of early retinal complications in diabetes. Invest Ophthalmol Vis Sci 2005;46:2210–2218. [PubMed: 15914643]

Budzilovich GN. Diabetic neuropathy complex. Virchows Arch A Pathol Anat 1970;350:105–122. [PubMed: 5310902]

Carroll SL, Byer SJ, Dorsey DA, Watson MA, Schmidt RE. Ganglion-specific patterns of diabetes-modulated gene expression are established in prevertebral and paravertebral sympathetic ganglia prior to the development of neuroaxonal dystrophy. J Neuropathol Exp Neurol 2004;63:1144–1154. [PubMed: 15581182]

Chan DC. Mitochondria: dynamic organelles in disease, aging, and development. Cell 2006;125:1241–1252. [PubMed: 16814712]

Chaparro RJ, Konigshofer Y, Beilhack GF, Shizuru JA, McDevitt HO, Chien YH. Nonobese diabetic mice express aspects of both type 1 and type 2 diabetes. Proc Natl Acad Sci U S A 2006;103:12475–12480. [PubMed: 16895987]

Choeiri C, Hewitt K, Durkin J, Simard CJ, Renaud JM, Messier C. Longitudinal evaluation of memory performance and peripheral neuropathy in the Ins2C96Y Akita mice. Behav Brain Res 2005;157:31–38. [PubMed: 15617768]

Duchen LW, Anjorin A, Watkins PJ, Mackay JD. Pathology of autonomic neuropathy in diabetes mellitus. Ann Intern Med 1980;92:301–303. [PubMed: 6243893]

Forehand CJ. Density of somatic innervation on mammalian autonomic ganglion cells is inversely related to dendritic complexity and preganglionic convergence. J Neurosci 1985;5:3403–3408. [PubMed: 4078634]

Frank S. Dysregulation of mitochondrial fusion and fission: an emerging concept in neurodegeneration. Acta Neuropathol (Berl) 2006;111:93–100. [PubMed: 16468021]

Hill CE, Hendry IA, Ngu MC, van Helden DF. Subpopulations of sympathetic neurones differ in their sensitivity to nerve growth factor antiserum. Brain Res 1985;355:121–130. [PubMed: 4075099]

Hill CE. Selectivity in sympathetic innervation during development and regeneration in the rat. Experientia 1985;41:857–862. [PubMed: 3891400]

Hopfner C, Pluot M, Caron J, Caulet T. [Morphological, optical and ultrastructural studies on the degenerative changes in the region of the lumbar sympathetic ganglia in the aged diabetic]. Pathol Eur 1971;6:122–136. [PubMed: 4111130]

Izumi T, Yokota-Hashimoto H, Zhao S, Wang J, Halban PA, Takeuchi T. Dominant negative pathogenesis by mutant proinsulin in the Akita diabetic mouse. Diabetes 2003;52:409–416. [PubMed: 12540615]

Jobling P, Gibbins IL. Electrophysiological and morphological diversity of mouse sympathetic neurons. J Neurophysiol 1999;82:2747–2764. [PubMed: 10561442]

Karbowski M, Youle RJ. Dynamics of mitochondrial morphology in healthy cells and during apoptosis. Cell Death Differ 2003;10:870–880. [PubMed: 12867994]

Kott I, Urca I, Sandbank U. Lumbar sympathetic ganglia in atherosclerotic patients, diabetic and nondiabetic. A comparative morphological and ultrastructural study Arch Surg 1974;109:787–792.

Leinninger GM, Backus C, Sastry AM, Yi YB, Wang CW, Feldman EL. Mitochondria in DRG neurons undergo hyperglycemic mediated injury through Bim, Bax and the fission protein Drp1. Neurobiol Dis 2006;23:11–22. [PubMed: 16684605]

Malik I, Turk J, Mancuso DJ, Montier L, Wohltmann M, Wozniak DF, Schmidt RE, Gross RW, Kotzbauer PT. Disrupted membrane homeostasis and accumulation of ubiquitinated proteins in a mouse model of infantile neuroaxonal dystrophy caused by PLA2G6 mutations. Am J Pathol 2008;172:406–416. [PubMed: 18202189]

Mathews CE, Langley SH, Leiter EH. New mouse model to study islet transplantation in insulin-dependent diabetes mellitus. Transplantation 2002;73:1333–1336. [PubMed: 11981430]

Parkman, HP.; Stapelfeldt, WH.; Miller, SM., et al. Enteric connection with peripheral sympathetic neurons. In: Tache, Y.; Wingate, DL.; Burks, FT., editors. Innervation of the Gut-Pathophysiological Implications. Boca Raton; CRC Press: 1994. p. 149-156.

Purves D, Lichtman JW. Geometrical differences among homologous neurons in mammals. Science 1985;228:298–302. [PubMed: 3983631]

Ron D. Proteotoxicity in the endoplasmic reticulum: lessons from the Akita diabetic mouse. J Clin Invest 2002;109:443–445. [PubMed: 11854314]

Rundles R. Diabetic neuropathy. General review with report of 125 cases Medicine 1945;24:111–160.

Schmidt RE. Neuropathology of human sympathetic autonomic ganglia. Microsc Res Tech 1996;35:107–121. [PubMed: 8923446]

Schmidt RE. Neuronal preservation in the sympathetic ganglia of rats with chronic streptozotocin-induced diabetes. Brain Res 2001;921:256–259. [PubMed: 11720733]

Schmidt RE. Age-related sympathetic ganglionic neuropathology: human pathology and animal models. Auton Neurosci 2002;96:63–72. [PubMed: 11911504]

Schmidt RE, Beaudet LN, Plurad SB, Dorsey DA. Axonal cytoskeletal pathology in aged and diabetic human sympathetic autonomic ganglia. Brain Res 1997;769:375–383. [PubMed: 9374210]

Schmidt RE, Dorsey DA, Beaudet LN, Frederick KE, Parvin CA, Plurad SB, Levisetti MG. Non-obese diabetic mice rapidly develop dramatic sympathetic neuritic dystrophy: a new experimental model of diabetic autonomic neuropathy. Am J Pathol 2003;163:2077–2091. [PubMed: 14578206]

Schmidt RE, Green KG, Feng D, Dorsey DA, Parvin CA, Lee JM, Xiao Q, Brines M. Erythropoietin and its carbamylated derivative prevent the development of experimental diabetic autonomic neuropathy in STZ-induced diabetic NOD-SCID mice. Exp Neurol 2008;209:161–170. [PubMed: 17967455]

Schmidt RE, McAtee SJ, Plurad DA, Parvin CA, Cogswell BE, Roth KA. Differential susceptibility of prevertebral and paravertebral sympathetic ganglia to experimental injury. Brain Res 1988;460:214–226. [PubMed: 2906265]

Schmidt RE, Parvin CA, Green KG. Synaptic ultrastructural pathology anticipates the development of neuroaxonal dystrophy in the sympathetic ganglia of aged and diabetic mice. J Neuropathol Exp Neurol. in press

Schmidt RE, Plurad SB, Parvin CA, Roth KA. Effect of diabetes and aging on human sympathetic autonomic ganglia. Am J Pathol 1993;143:143–153. [PubMed: 8317545]

Schmidt RE, Summerfield AL, Hickey WF. Ultrastructural and immunohistologic characterization of guanethidine-induced destruction of peripheral sympathetic neurons. J Neuropathol Exp Neurol 1990;49:150–167. [PubMed: 2307981]

Semra YK, Smith NC, Lincoln J. Comparative effects of high glucose on different adult sympathetic neurons in culture. Neuroreport 2004;15:2321–2325. [PubMed: 15640748]

Semra YK, Wang M, Peat NJ, Smith NC, Shotton HR, Lincoln J. Selective susceptibility of different populations of sympathetic neurons to diabetic neuropathy in vivo is reflected by increased vulnerability to oxidative stress in vitro. Neurosci Lett 2006;407:199–204. [PubMed: 16973273]

Shotton HR, Clarke S, Lincoln J. The effectiveness of treatments of diabetic autonomic neuropathy is not the same in autonomic nerves supplying different organs. Diabetes 2003;52:157–164. [PubMed: 12502507]

Silos-Santiago I, Molliver DC, Ozaki S, Smeyne RJ, Fagan AM, Barbacid M, Snider WD. Non-TrkA-expressing small DRG neurons are lost in TrkA deficient mice. J Neurosci 1995;15:5929–5942. [PubMed: 7666178]

Yoshioka M, Kayo T, Ikeda T, Koizumi A. A novel locus, Mody4, distal to D7Mit189 on chromosome 7 determines early-onset NIDDM in nonobese C57BL/6 (Akita) mutant mice. Diabetes 1997;46:887–894. [PubMed: 9133560]

Zochodne DW, Ramji N, Toth C. Neuronal targeting in diabetes mellitus: A story of sensory neurons and motor neurons. Neuroscientist 2008;14:311–318. [PubMed: 18660461]

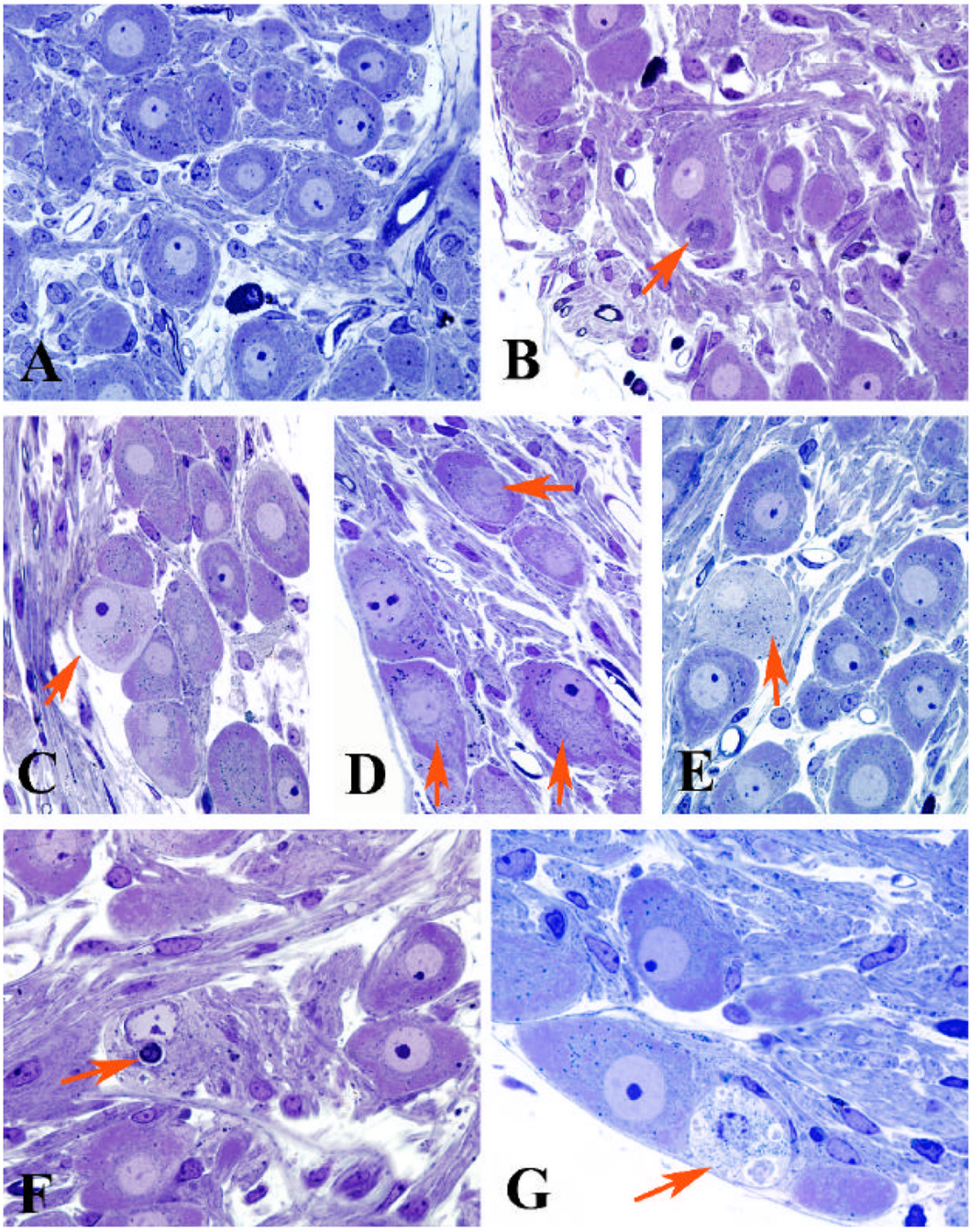

Figure 1.

Light microscopic appearance of the SMG and CG of control and diabetic Akita mice

A) Principal sympathetic neurons surrounded by neuropil with occasional mast cells (control SMG, 5 months of age)

B) A typical dystrophic neurite (arrow) is intimately associated with an adjacent cell body (2 month diabetic CG)

C–E) Neurons show patchy loss of Nissl substance involving the subplasmalemma (arrow, C), central perinuclear area (arrows, D) and entire perikaryon (arrow, E) [C, 4 month diabetic CG; D, 8 month diabetic SMG; E, 8 month diabetic CG]

F,G) Degenerating neurons may contain large membranous aggregates (arrow, F) or disintegrating cytoplasm (arrow, G) [F, 2 month diabetic CG; G, 4 month diabetic SMG] (original magnification A–G, 500X)

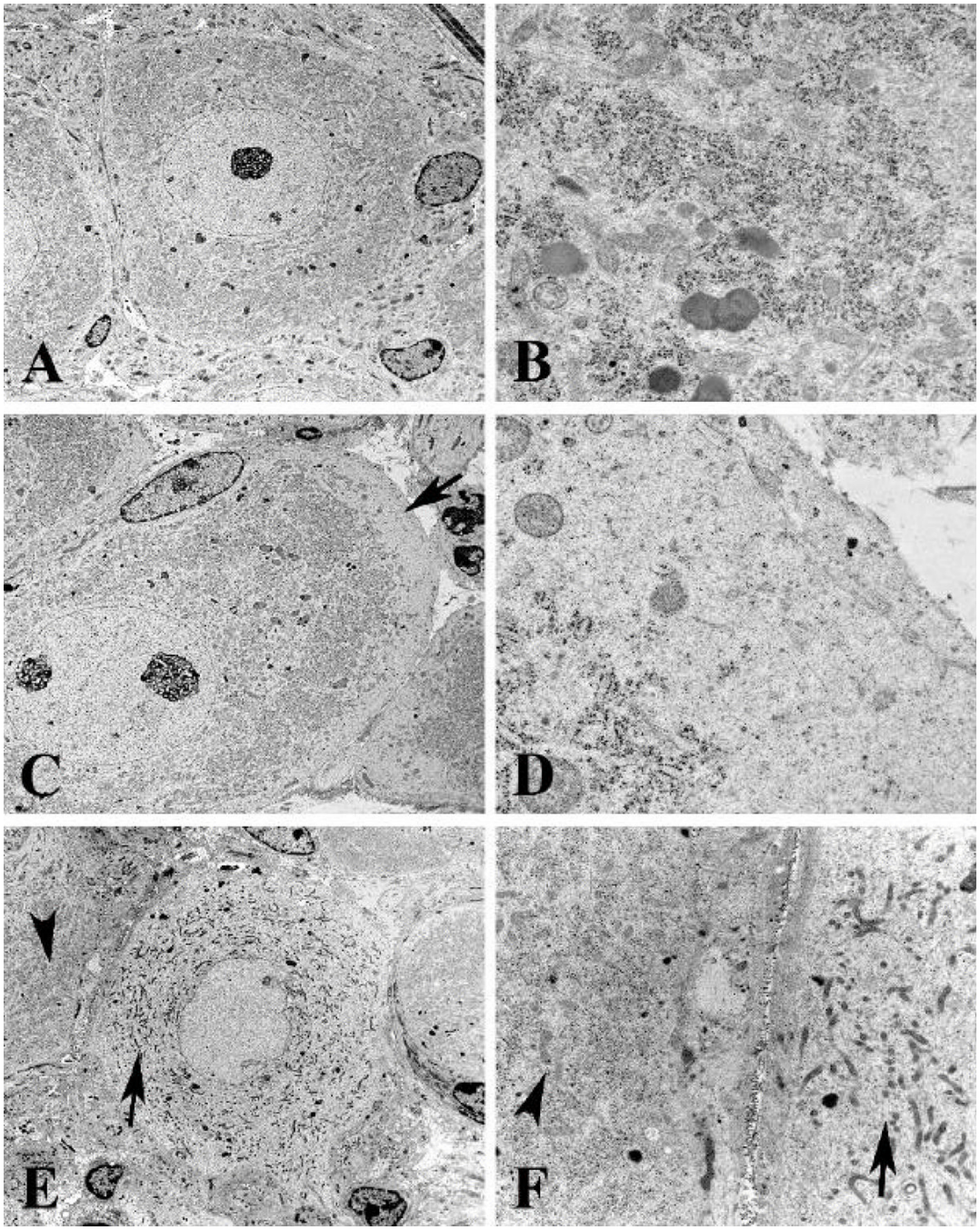

Figure 2.

Ultrastructural appearance of rough endoplasmic reticulum in the CG of control and Akita mice diabetic for 2 months

A,B) Control CG neuron shows a round nucleus with little heterochromatin and a prominent nucleolus with discrete collections of rough endoplasmic reticulum (B). [A, CG, 9 months of age; B, 5 month age SMG] (original magnification: A, 3000X; B, 25000X)

C,D) Subplasmalemmal loss of rough endoplasmic reticulum (arrows, C,D) with little additional pathology is a frequent pattern in diabetic Akita neurons. [C,D, 8 month diabetic CG] (original magnification: C, 4000X; D, 30000X)

E,F) Complete loss of perikaryal rough endoplasmic reticulum is shown (arrow, E) in comparison to an adjacent neuron with a normal pattern (arrowhead, E). The pale neuronal cytoplasm (arrow, F) contains mitochondria smaller than those of the adjacent normal neuron (arrowhead, F). [4 month diabetic SMG] (original magnification: E, 3000X; F, 12000X)

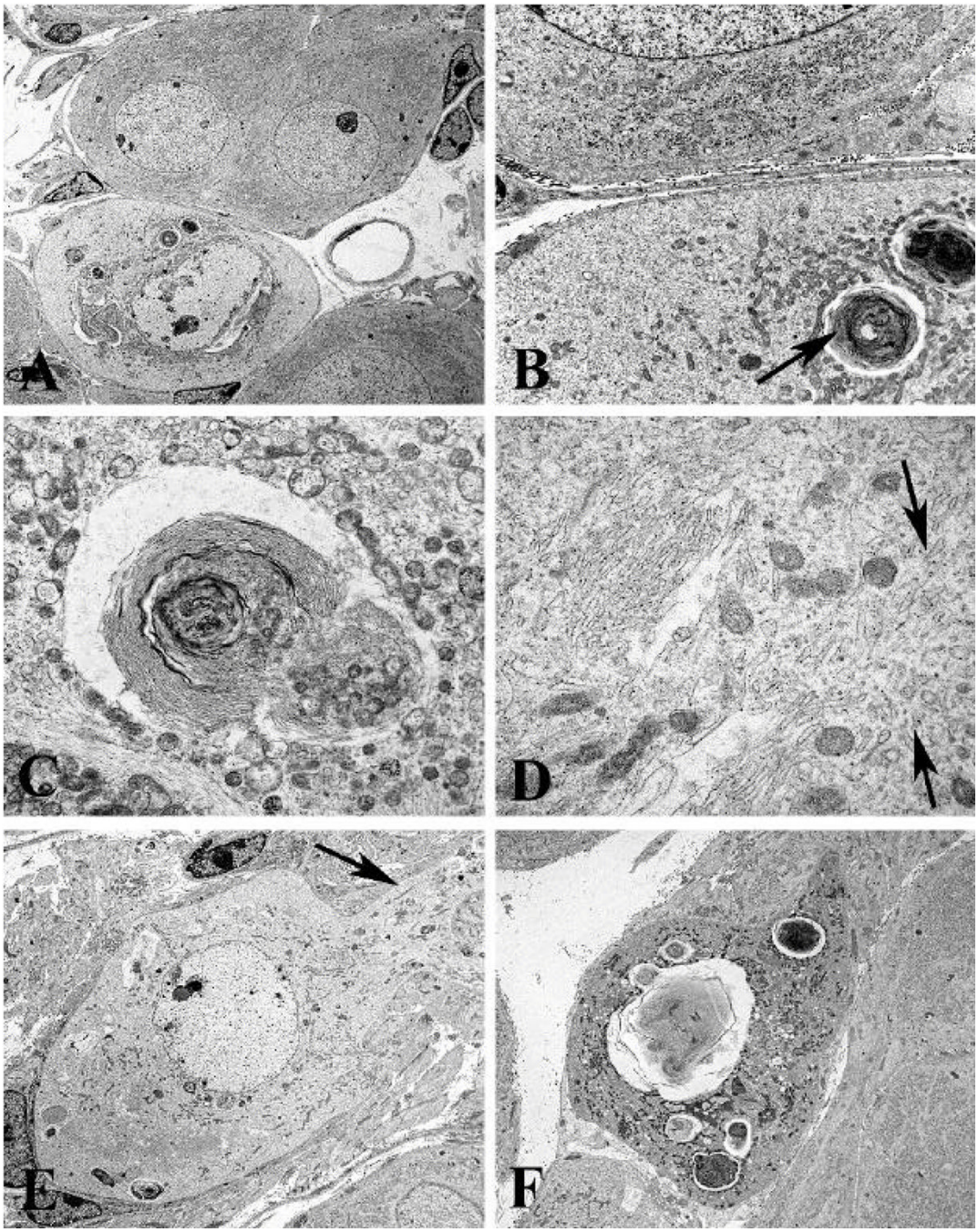

Figure 3.

Ultrastructural appearance of membranous pathology involving the CG of Akita mice diabetic for 2 months

A–C) A degenerating neuron containing large membranous aggregates (A), is shown at higher magnification in B and C, and is accompanied by large numbers of minute mitochondria. (original magnification: A, 2500X; B, 12000X; C, 20000X)

D) Pale cytoplasm shows large numbers of membranous elements (arrows) without attached ribosomes (original magnification: 40000X)

E) Neuronal pallor extends into adjacent proximal dendrite (arrows) (original magnification: 3000X)

F) Terminal appearance of degenerating neuron (original magnification: 4000X)

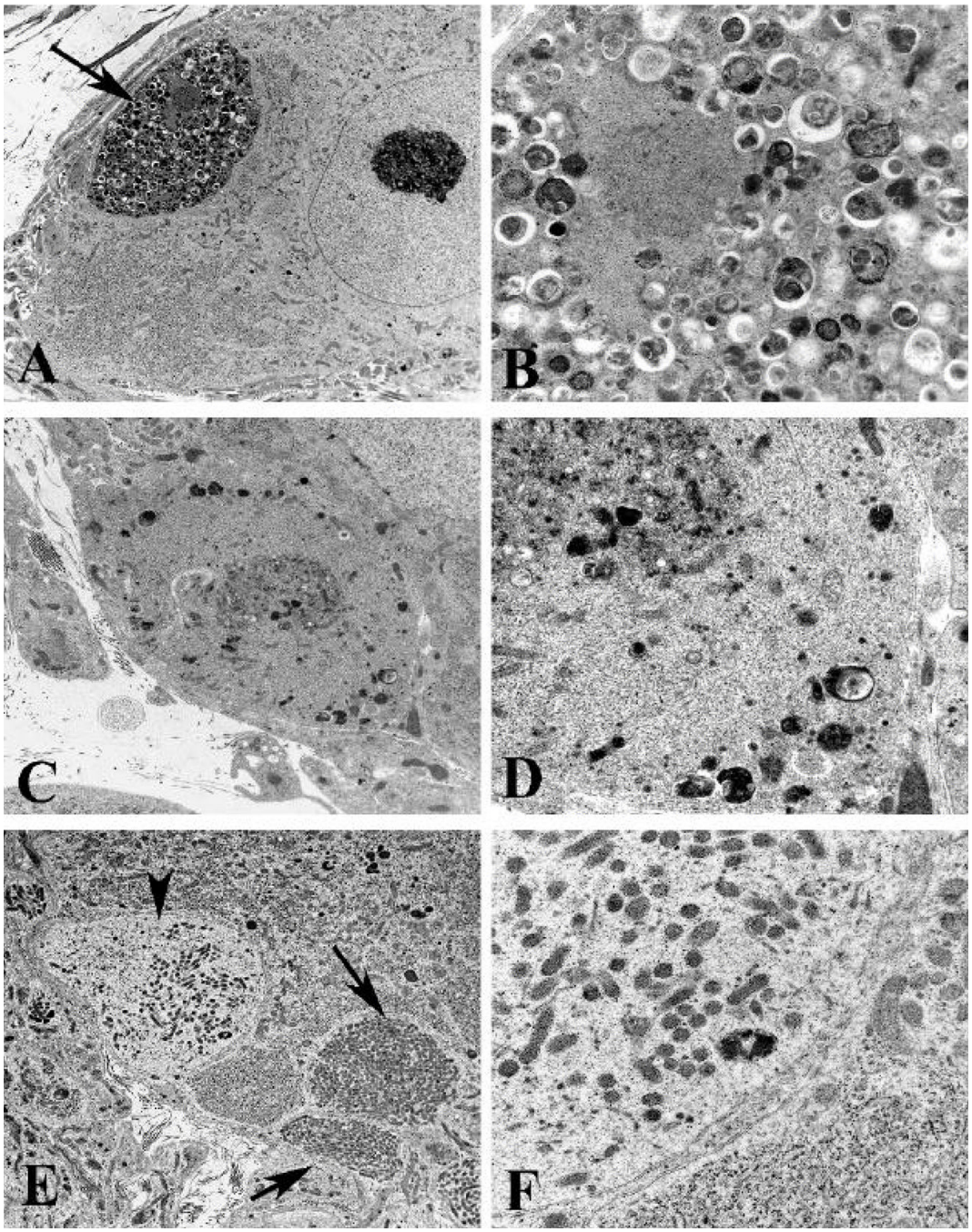

Figure 4.

Ultrastructural appearance of neuritic dystrophy in the SMG and CG of Akita mice

A,B) Axonal nerve terminal (arrow, A) containing numerous normal and degenerating organelles, and autophagosomes shown at higher magnification in B. [8 month diabetic SMG] (original magnification: A, 5000X; B, 25000X)

C,D) Swollen terminal axon with aggregated normal, degenerating and autophagic organelles embedded in disorganized cytoskeleton, seen at higher magnification in D. [4 month diabetic SMG] (original magnification: C, 10000X; D, 25000X)

E,F) Dilated dendrites containing large numbers of small mitochondria (arrows, E) and a pale dendritic process (arrowhead, E) containing small mitochondria, tubulovesicular elements and

little rough endoplasmic reticulum (F) [8 month diabetic CG] (original magnification: E, 6000X; F, 25000X)

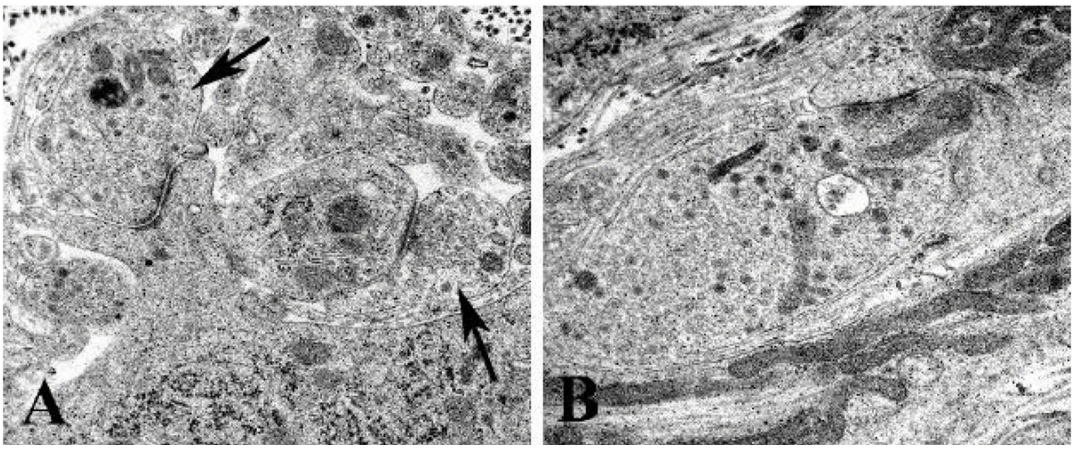

Figure 5.

Ultrastructural appearance of typical nerve terminals in control and Akita mouse CG

A,B) Typical axonal terminals (arrows, A) forming synapses on a dendrite and a perikaryal spine in a control mouse. The presynaptic nerve terminals of Akita mice (B) are typically larger than those of controls although the material accumulated consists of typical synaptic vesicles and mitochondria [A, 3 months of age; B, 4 month diabetic] (original magnification: A,B, 40000X)

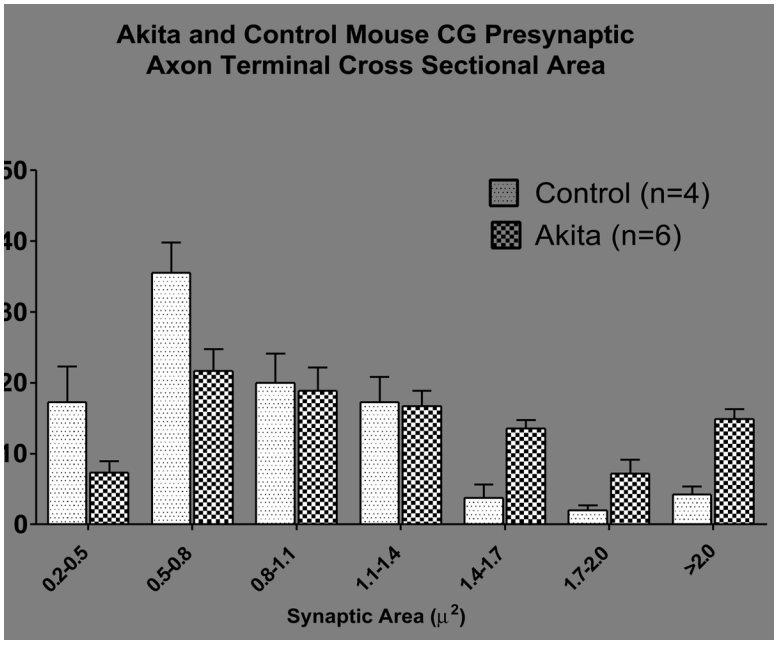

Figure 6.

Size-frequency plot of the distribution of presynaptic axon terminal cross sectional areas in the CG of control and Akita mice diabetic for 8 months. Values represent the means + SEM of 4 control and 6 Akita mice ganglia.

Table 1

Akita and Control Mouse Metabolic Parameters

Experimental Group	Body Weight (g)	Plasma Glucose (mg/dl)
2 months		
Control (n=3)	23 ± 0.6	---
Diabetic (n=4)	27.7 ± 1.8	558 ± 24
4 months		
Control (n=3)	33 ± 0.7	191 ± 14
Diabetic (n=7)	24.7 ± 1.1*	560 ± 19*
8 months		
Control (n=4)	30.4 ± 1.7	---
Diabetic (n=5)	21 ± 2*	>600

Values represent the means ± SEM of the plasma glucose and body weights at sacrifice of n age-matched control and Akita mice of several diabetic durations.

* Statistical Comparison: $p \leq 0.001$

Table 2

Frequency of Pale Neurons in Akita and Control Mouse Prevertebral Sympathetic Ganglia

Group	Duration of Diabetes (months)	Pale Neuron Frequency (%)
CG		
Control (n=3)	2	0+0
Diabetic (n=4)		1.95 + 0.6[#]
CG	4	
Control (n=4)		0 + 0
Diabetic (n=3)		7.0 + 1.3
CG	8	
Control (n=4)		0 + 0
Diabetic (n=6)		1.9 + 0.5[#]

Values represent the means ± SEM of the percentage of pale neurons in the CG from n age-matched control and Akita mice diabetic for 2, 4 or 8 months.

[#]Statistical Comparison: $p \leq 0.05$ in comparison with 4 month diabetic CG

Table 3

Effect of Duration of Diabetes on the Frequency of Neuritic Dystrophy in Akita and Control Mouse Sympathetic Ganglia

Group	Duration of Diabetes	Dystrophic Neurites (#/neuron)
SMG		
Control (n=3)	4 months	0.05 ± 0.02
Diabetic (n=5)		0.72 ± 0.08*
Celiac		
Control (n=3)	2 months	0.03 + 0.02
Diabetic (n=4)		0.39 + 0.08#
Control (n=3)	4 months	0.02 ± 0.01
Diabetic (n=4)		0.98 ± 0.04*
Control (n=4)	8 months	0.06 + 0.02
Diabetic (n=6)		1.32 + 0.24*
SCG		
Control (n=3)	4 months	0.01 ± 0.01
Diabetic (n=4)		0.01 ± 0.01
Control (n=4)	8 months	0.01 ± 0.01
Diabetic (n=4)		0.02 ± 0.02

Values represent the means ± SEM of the frequency of neuritic dystrophy sampled in the SMG, CG and SCG from n age-matched control and Akita mice diabetic for 2–8 months.

* Statistical Comparison: $p \leq 0.003$;

# $p < 0.01$

Table 4

Mean Presynaptic Axon Terminal Cross Sectional Area of Akita and Control Mouse Pre- and Paravertebral Sympathetic Ganglia

Experimental Group	Number of Examined Synapses	Mean Synapse Area (μ^2)
SMG		
4 months		
Control (n=3)	59 ± 11	1.05 ± 0.07
Diabetic (n=4)	66 ± 8	1.39 ± 0.11[#]
CG		
4 months		
Control (n=3)	41 ± 12	0.86 ± 0.03
Diabetic (n=4)	44 ± 4	1.33 ± 0.11[*]
8 months		
Control (n=4)	44 ± 5	0.88 ± 0.01
Diabetic (n=6)	40 ± 8	1.31 ± 0.05[*]
SCG		
4 months		
Control (n=3)	54 ± 5	1.18 ± 0.03
Diabetic (n=4)	41 ± 4	0.86 ± 0.03[*]
8 months		
Control (n=4)	41 ± 6	.90 ± 0.03
Diabetic (n=4)	52 ± 4	.90 ± 0.05

Values represent the means ± SEM of the presynaptic axon terminal cross sectional area sampled in the prevertebral superior mesenteric (SMG) and celiac (CG) and paravertebral chain superior cervical (SCG) ganglia from n age-matched control and Akita (Diabetic) mice diabetic for 4 or 8 months.

[*] Statistical Comparison: $p \leq 0.001$;

[#] $p \leq 0.05$